AIAA AVIATION Forum
June 27-July 1, 2022, Chicago, IL & Virtual
AIAA AVIATION 2022 Forum

10.2514/6.2022-4153

Examination of Derived Gust Velocities from C-130 in Forest Service Operation

Linda K. Kliment[1], Kamran Rokhsaz[2], and Syed Junaid Ali[3]
Wichita State University, Wichita, KS 67260-0042, USA

John A. Nelson[4]
United States Forest Service, Boise, ID 83705, USA

Flight data from two EC-130Q and two L-382G airframes being flown as airtankers in USFS operations were analyzed. Firefighting flights were separated into five phases: cruise 1, entry, drop, exit, and cruise 2. The recorded normal accelerations were used to calculate the derived gust velocities and the results were presented for each phase. Results showed that the frequency of the atmospheric gusts were dependent on MSL altitude. Because the cruise phases were flown at higher altitudes, the derived gust velocities occurred more frequently for the entry, drop, and exit phases. Likewise, derived gust velocities occurred more frequently for the firefighting missions due to the ferry flights occurring at higher altitudes. The results presented in this paper compared favorably with those observed for other airtankers.

I. Introduction

AERIAL support plays an important role in helping to slow the spread of forest fires. This role carries more importance as fires increase in intensity. In areas of rough terrain, the aerial delivery of retardant can begin to slow the growth of the fire before ground crews arrive in order keep fires smaller [1]. Due to the importance of aerial support, United States Forest Service (USFS) has been focused on the health of the airtankers flying under contract with them as well as the modernization of the fleet [2].

United Stated Forest Service (USFS) began a monitoring program in 2004 following the loss of two airtankers [3]. As part of this program, every airtanker flying in support of USFS operations is required to have a Digital Flight Data Recorder (DFDR) and record the accelerations experienced by the airframe as well as other parameters. The data is proprietary to the airplane operators. This data is made available to USFS to determine the operational flight loads spectra [4] along with usage information for the airframe.

USFS first analyzed the data for the P-2V and P-3A legacy airtankers due to their concerns about the age of the fleet [5]. This was followed by a study of the Beechcraft King Air twin turboprops [6, 7]. While the King Airs are not airtankers, they are flown in a variety of support roles in firefighting operations. Recently, the focus has turned to the next-generation airtankers which are replacing legacy airtankers [2]. Type 1 next-generation large airtankers have a retardant capacity greater than 3,000 gallons and are faster and more cost-effective than legacy airtankers [2]. A study of the BAe-146 and RJ-85 aircraft has been completed [8, 9]. This was followed by an exploratory study of the MD-87 and DC-10 aircraft. Currently, the C-130 aircraft are being analyzed.

The C-130 airtankers are contracted or operated by the US Air Force through the MAFFS program [10]. Through the Air Force, the C-130 is equipped with a Modular Airborne FireFighting System (MAFFS) which can be loaded quickly into the airplane. The contracted C-130 is equipped with a 4,000 gallon tank system. The focus of the current results are on those that are contracted. The C-130 aircraft was of interest to USFS in the modernization of their fleet due to the fact that it was originally designed for maneuver load factors that are similar to those experienced during firefighting operations [2].

[1] Associate Professor, Department of Aerospace Engineering, Senior Member AIAA.
[2] Professor, Department of Aerospace Engineering, Associate Fellow AIAA.
[3] Graduate Research Assistant, Department of Aerospace Engineering.
[4] Airworthiness Branch Chief, Fire and Aviation Management.

II. Method of Analysis

A. Flight Data

The flights on which the results in this article are based were recorded on two EC-130Q airframes [11, 12] and two L-382G airframes [13]. Information for these two airplanes, as they are used as airtankers, is shown in Table 1. The DFDR recorded information in a uniform 32-Hz format. After it was recorded, the data was stored in a central library which could be accessed by USFS and the operators. There were some subtle differences between the data from each airframe as well as between years. Therefore, before it was used, the data was put in a standard format which is shown in Table 2. At the same time, anomalous data was corrected. This included replacing dropped signals and eliminating flights with unrealistic values in important channels. During this step, it was determined that the pitch and roll angles were incorrect for a majority of the flights. Therefore, results which required these angles were not found.

B. Takeoff and Landing Determination

Only airborne phases were analyzed for this study. The weight-on-wheels signal recorded by the DFDR was used to determine the takeoff and landing points. The flight duration was defined as the time from the liftoff to the touchdown and the flight distance was found by integrating GPS airspeed.

C. Filtering of the Normal Acceleration

Normal, longitudinal, and lateral accelerations were recorded at a constant 32 Hz. However, it was apparent that the normal acceleration included information relating to the structural modes of the airplane. Therefore, in all analysis related to USFS operations in which the data was recorded at 32 Hz, the normal accelerations were filtered in order to remove information due to structural vibration. In order to remain consistent with previous USFS studies, an 8^{th} order Butterworth filter with 8-Hz cut-off frequency was used.

D. Converting Flap Deflection Percentage into Detents

Flap position was used in order to separate flight phases. For the C-130, the flap position was recorded in percent deflection. This was converted into detents using the following definitions

- First detent: 10%-40%
- Second detent: 40%-50%
- Third detent: 50%-60%
- Fourth detent: 60%-100%

For reference, during takeoff the flaps were commonly 50% deflected. During retardant drops and landings, the flaps were commonly 100% deflected.

E. Phase Separation

The firefighting flights were separated into phases so that the results could be presented for each. The cruise 1 and 2 phases were those to and from the fire zone, respectively. These phases contained the maximum altitude for the firefighting flight. There was only one each of the cruise phases per flight. The number of entry, drop, and exit phases depended on the number of retardant drops there were during the flight. While most flights contained a single retardant drop, there were still many that had more than one. The drop phase was determined by the time during which the bay door was open. The entry and exit phase lengths were based on either elapsed time or changes in the flap detent. The criteria used to separate the phases is shown in Table 3. Note that the ferry/maintenance flights were not separated into phases and the start and end time was based on the takeoff and landing.

Table 1. Airplane Characteristics in USFS Service

Parameter	EC-130Q [14]	L-382G [13]
Wing Span (ft)	132.6	132.6
Overall Length (ft)	99.5	112.8
Maximum Takeoff Weight (lb)	155,000	155,000
Maximum Landing Weight (lb)	155,000	135,000
Retardant Capacity, Tanked (gal)	4,000	4,000

Table 2. Data Channels Available for the Analysis

Channel	Parameter	Channel	Parameter
1	Line Number	19	Static Pressure (psf)
2	Elapsed Time (seconds)	20	Outside Air Temperature (Celsius)
3	Latitude (degrees)	21	Cabin Pressure Differential (psi)
4	Longitude (degrees)	22-24	Indicated, Equivalent, True Airspeed (knots)
5	Heading (degrees)	25	Weight on Wheels (binary)
6	GPS Altitude (feet)	26	Flap Position (percentage)
7	Pressure Altitude (feet)	28	Tank Door (binary)
8	Ground Speed (knots)	29	Fuel Weight (lb)*
9	GPS Vertical Speed (fpm)	30	Retardant Weight (lb)
10-12	Longitudinal, Lateral, Normal Accel. (g)	31	Gross Weight (lb)*
13, 15	Pitch and Roll (degrees)	32	CG Acceleration (g)*
14, 16-17	Pitch Rate, Roll Rate, Yaw Rate (deg/s)	33	Terrain Elevation (feet)[+]
18	Pitot Pressure (psf)		

* Available on select flights.
[+] Added using USGS National Elevation Database and the latitude and longitude recorded by the DFDR.

Table 3. Flight Phase Separation Criteria

Flight Phase	Start Time Identification	End Time Identification
Cruise 1	One minute after takeoff	Three minutes before the start of the first drop
Entry	Flaps lowered prior to start of the drop or three minutes before the opening of the tank door	Opening of the first tank door
Drop	Opening of the tank door	Closing of the tank door plus 0.5 second
Exit	End of the drop	Two flap movements after the end of the drop or ninety seconds after the end of the drop
Cruise 2	Three minutes after the end of the last drop or one minute after takeoff for ferry/maintenance flights	One minute before landing

F. Weight Estimation

All recorded data contained the retardant weight. However, only the L-382G data also contained fuel and aircraft instantaneous weight. Even then, only one L-382G airframe had an instantaneous weight which showed the effect of the retardant release. Analysis of the reliable weight information resulted in parameters that could be used to make estimations. These parameters included average aircraft, fuel, and retardant weights at takeoff. The average fuel burn rate was determined using weights at takeoff and landing. The parameters that were used to estimate instantaneous weight are shown in Table 4. While this technique resulted in acceptable instantaneous aircraft weight for firefighting missions, its effectiveness for other missions was questionable.

Table 4. Parameters for Weight Estimation

Parameter	Value
Aircraft Takeoff Weight (lb)	135,000
Fuel Weight at Takeoff (lb)	16,000
Retardant Weight at Takeoff (lb)	35,000
Fuel Burn Rate (lb/s)	1.5

G. Derived Gust Velocity Calculation

Derived gust velocities were calculated from recorded normalized normal accelerations due to gusts.

$$U_{de} = \frac{\Delta n_z}{\bar{C}} \tag{1}$$

where:

U_{de} = derived gust velocity (ft/s)
Δn_z = incremental vertical load factor (g)

The aircraft response factor, $\bar{C}$, was calculated from

$$\bar{C} = \frac{\rho_0 V_e C_{L_\alpha} S}{2W} K_g \tag{2}$$

where:

ρ_0 = 0.002377 slug/ft^3, standard sea level air density
V_e = equivalent airspeed (ft/s)
C_{L_α} = aircraft lift-curve slope (per radian)
S = wing reference area (ft^2)
W = instantaneous aircraft weight (lb)
K_g = $\frac{0.88\mu}{5.3+\mu}$, gust alleviation factor
μ = $\frac{2W}{\rho g \bar{c} C_{L_\alpha} S}$, reduced mass
ρ = air density at altitude from $\rho = \frac{P}{\bar{R}T}$, (slug/ft^3)
g = 32.17 ft/s^2, acceleration of gravity
$\bar{c}$ = wing mean geometric chord (ft)
P = static pressure, recorded by DFDR (psf)
$\bar{R}$ = 1,716.3 ft-lb/slug-R, specific gas constant for air
T = absolute temperature, recorded by DFDR (°R)

From reference 15, aircraft lift-curve slope, C_{L_α}, was determined as

$$C_{L_\alpha} = C_{l_{\alpha,wb}} \left[1 + \frac{C_{l_{\alpha,t}}}{C_{l_{\alpha,wb}}} \frac{S_t}{S} \left(1 - \frac{\partial \varepsilon}{\partial \alpha} \right) \right] \tag{3}$$

where:

$C_{l_{\alpha,wb}}$ = wing lift-curve slope (per radian)
$C_{l_{\alpha,t}}$ = horizontal tail lift-curve slope (per radian)
S_t = horizontal tail area (ft^2)
S = wing area (ft^2)
$\frac{\partial \varepsilon}{\partial \alpha}$ = rate of change of downwash angle at the tail due to the wing [16]

$$\frac{\partial \varepsilon}{\partial \alpha} \approx \frac{0.349 C_{l_{\alpha,wb}}}{\lambda^{0.3} A_r^{0.725}} \left(\frac{3\bar{c}}{l_t'} \right)^{0.25} \tag{4}$$

where:

λ = wing taper ratio
A_r = wing aspect ratio
$\bar{c}$ = wing mean geometric chord (ft)
l_t' = distance between the wing and the horizontal tail aerodynamic centers (ft)

From reference 17, lift-curve slopes of individual lifting surfaces were found assuming thin airfoils with lift-curve slopes of 2π per radian according to equation 5.

$$\left(C_{l_\alpha}\right)_{\text{Wing or tail}} = \frac{2\pi A_r}{2+\sqrt{\left[4+A_r^2\beta^2\left(1+\frac{\tan^2\Lambda}{\beta^2}\right)\right]}} \tag{5}$$

In equation 5:

A_r = b^2 / S , aspect ratio
b = span (ft)
β = $\sqrt{1-M^2}$, compressibility effect
M = V_t / a , flight Mach number
Λ = wing half-chord sweep angle (degrees or radian)
V_t = true airspeed (ft/s)
a = $\sqrt{\gamma \bar{R} T}$, local speed of sound (ft/s)
γ = 1.4, ratio of specific heat constants for air

III. Results and Discussion

Derived gust velocities were determined per nautical mile and categorized in MSL altitude bands that are shown in Table 5. The distances for the phases and flights are shown in the same table. The results are presented first by the GAG flights and followed by the phases for the firefighting missions.

Shown in Figure 1 are the cumulative occurrences of the derived gust velocity for all firefighting missions. Altitude dependence could be clearly seen, although there was little difference between the results of the third and fourth altitude bands. The results for the lower MSL altitude bands were dominated by data from the entry, drop, and exit phases. Those for the higher altitude bands were dominated by the cruise phases. In no case were the airplanes flown in the highest altitude band for the firefighting missions. The lowest and seventh altitude bands had very little data and therefore the results had more scatter.

The cumulative occurrences of the derived gust velocity for all ferry/maintenance missions are shown in Figure 2. Theoretically, the type of mission should not have an effect on the derived gust velocities, which represent the atmospheric turbulence content. However, there are differences between the results of Figures 1 and 2, most obvious in the lower altitude bands. This could be due to the fact that the ferry/maintenance results were based on very little data in the lowest altitude band.

Table 5. Distances for Phases and Flights in Altitude Bands

Altitude Band Ceiling	Distance (nm)						
	Cruise 1	Cruise 2	Entry	Drop	Exit	Firefighting Phases	Ferry/ Maintenance
500	9.3	39.9	6.2	3.7	14.3	73.3	69.0
1500	1,197.2	1,086.6	136.4	41.3	258.3	2,719.7	1,212.5
4500	16,247.2	12,118.0	1,218.5	181.9	1,638.8	31,404.4	4,918.1
9500	43,050.9	23,512.0	1,846.8	228.2	2,467.5	71,105.4	5,505.5
14,500	32,361.1	17,726.1	177.7	7.9	154.0	50,426.8	4,077.2
19,500	103.8	5,535.4	12.2	0.3	3.2	5,654.9	2,477.7
24,500	264.1	658.2	2.5	0	0	924.8	1,754.2
35,000	0	0	0	0	0	0	3,638.1
Total	93,233.6	60,676.1	3,400.3	463.2	4,536.2	162,309.3	23,652.2

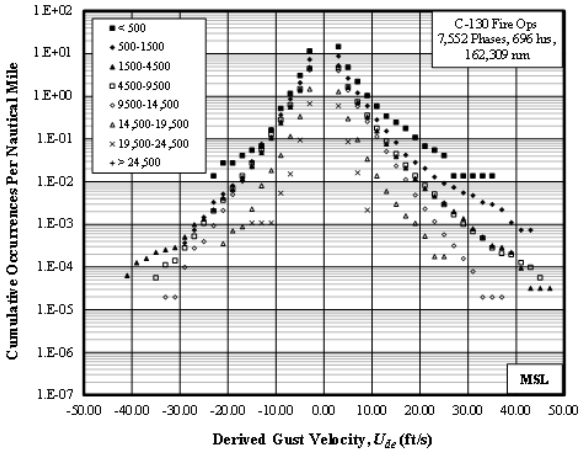

Fig. 1 Derived Gust Velocity, Firefighting Missions

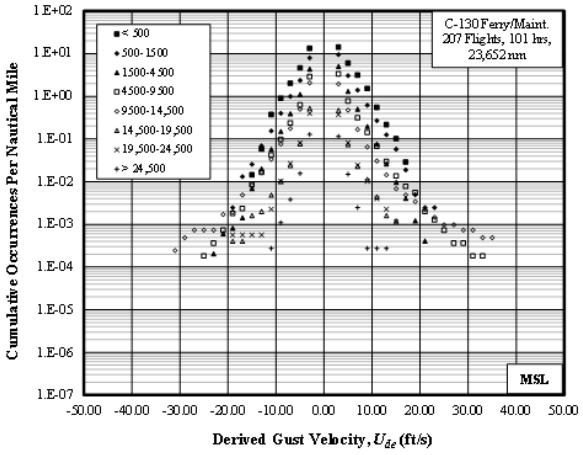

Fig. 2 Derived Gust Velocity, Ferry/Maintenance

The results for the cruise phases are shown in Figures 3 and 4. Cruise phases were typically flown at higher MSL altitudes and the results tend to match those for the higher altitude bands of Figure 1. The results from the two cruise phases differ slightly, which could be due to the way that the weights were estimated.

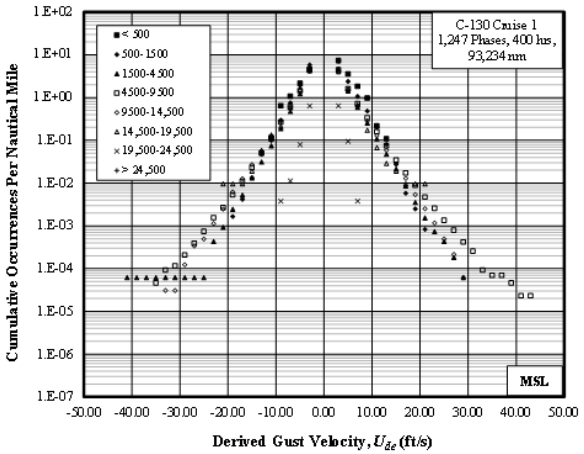

Fig. 3 Derived Gust Velocity, Cruise 1

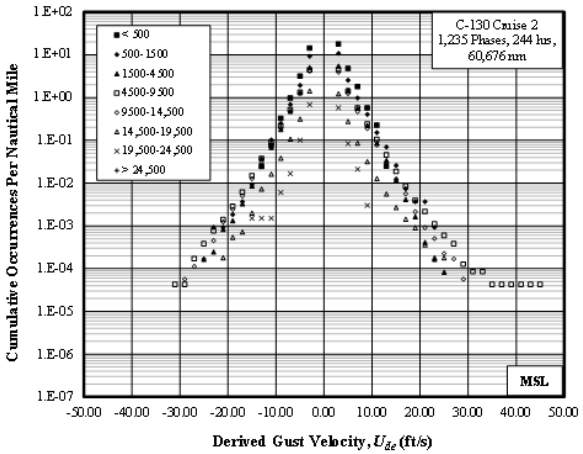

Fig. 4 Derived Gust Velocity, Cruise 2

The results for the entry, drop, and exit phases are shown in Figures 5-7. These phases were flown at lower MSL altitudes. The derived gust velocities for these three phases were two to three magnitudes larger than those of the cruise phases.

Shown in Figure 8 is a comparison of the firefighting phases without consideration of altitude bands. The drop phases, which were flown at the lowest altitudes, had the highest frequencies of occurrence. This was followed by the entry and exit phases. The cruise phases had the lowest frequencies of occurrence due to being flown at higher altitudes.

Presented in Figures 9 and 10 are comparisons. Figure 9 shows the comparison of cumulative occurrence of the derived gust velocity for different C-130 missions. Ferry and maintenance flights were flown at relatively higher altitude and, therefore, exhibited lower frequencies of occurrence. On the other hand, firefighting missions are flown at lower altitudes resulting in derived gust velocities that were one order of magnitude more frequent. These results are consistent with those from the BAe-146/RJ-85. Shown in Figure 10 is a comparison of the C-130 results with the BAe-146/RJ-85 USFS operations and Boeing 747 commercial operations [18]. The results for the Boeing 747 were presented by flap setting. Since the flap deflection is not expected to influence the derived gust velocities, the differences between the two cases can be attributed to predominant altitudes in which the aircraft were flown. In

commercial operations, it is expected that the aircraft would be at lower altitudes, near takeoff and landing, when the flaps were deflected. It is clear from Figure 10 that the aircraft flown in support of USFS missions are subjected to higher levels of atmospheric turbulence. The commercial operations occur at higher altitudes and are flown to avoid turbulence for ride comfort.

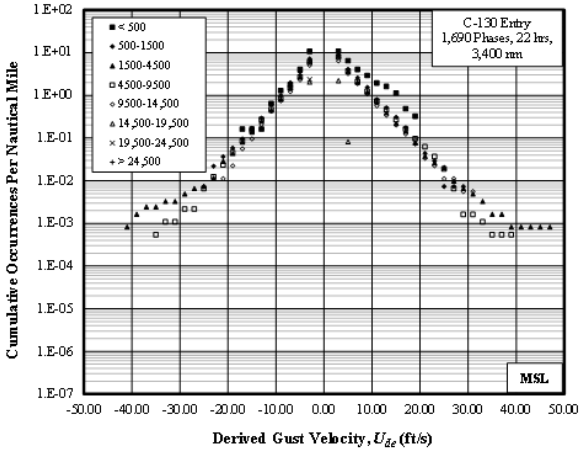

Fig. 5 Derived Gust Velocity, Entry

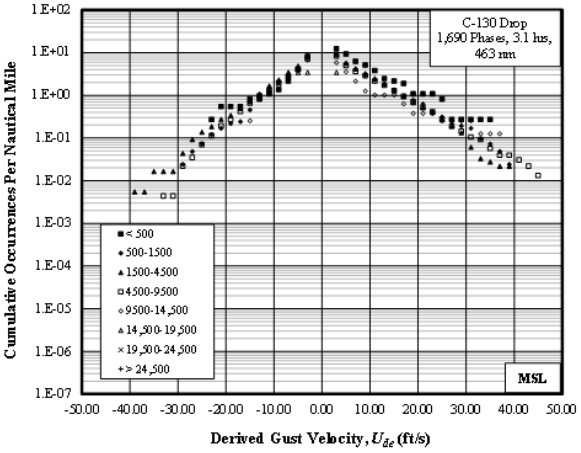

Fig. 6 Derived Gust Velocity, Drop

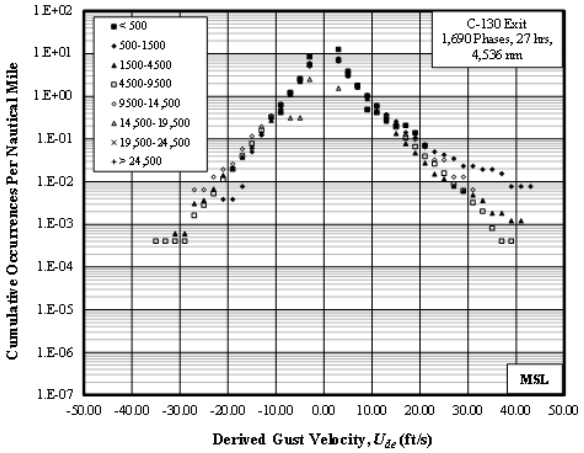

Fig. 7 Derived Gust Velocity, Exit

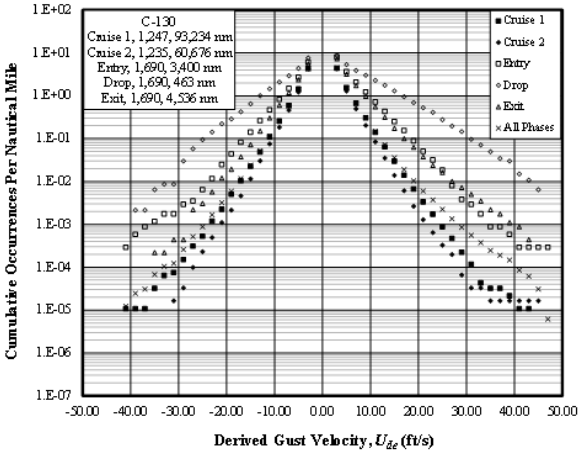

Fig. 8 Derived Gust Velocity, All Phases

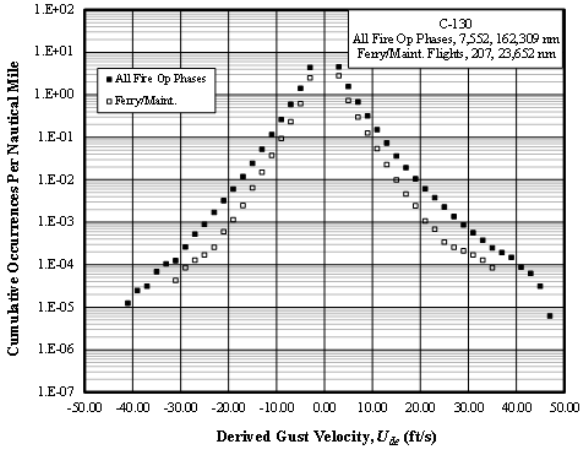

Fig. 9 Derived Gust Velocity, Flight Type Comparison

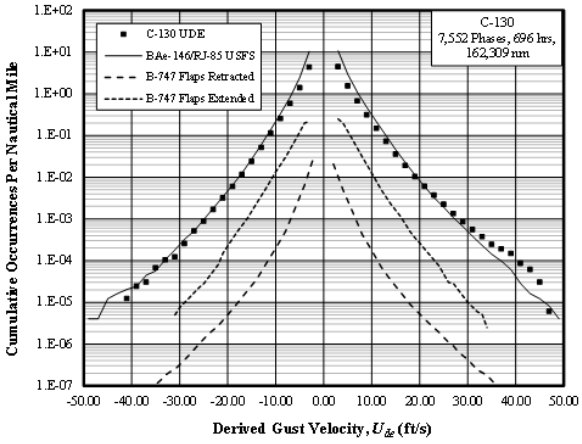

Fig. 10 Derived Gust Velocity, Comparisons

IV. Conclusions

Recorded flight data was available for two EC-130Q and two L-382G airframes flying in support of US Forest Service firefighting operations. Derived gust velocities were calculated from the recorded normal accelerations. In order to do this, the instantaneous weight was estimated. Firefighting flights were separated into five phases: cruise 1, entry, drop, exit, and cruise 2. Cumulative occurrences of derived gust velocities were presented for each phase in MSL altitude bands. The results were normalized per nautical mile.

The phase results showed a correlation of frequencies with MSL altitude. The results for the firefighting phases were compared and it was shown that the highest frequencies of occurrence were associated with the drop phase, followed by the entry and exit. This was attributed to the cruise phases being flown at higher altitudes. A comparison of the firefighting and ferry/maintenance missions was made and the derived gust velocities were shown to occur more frequently for the former. This was consistent with the results for other airtankers. A comparison was made with commercial operations and the current results exhibited higher and more frequent gust velocities. These results were also consistent with that observed in previous studies of other airtankers.

Acknowledgement

This effort was funded by the United States Forest Service through the Grant 17-G-004 administered by the Federal Aviation Administration. The authors wish to recognize the support and the guidance provided by Mr. David Rathfelder from Los Angeles Aircraft Certification Office and Ms. Heather Castillo from United States Forest Service in conducting this work. The FAA project monitor was Dr. Sohrob Mottaghi.

References

[1] Standards for Airtanker Operations, USDA Forest Service, July 2019.
[2] Large Airtanker Modernization Strategy, USDA Forest Service, Final Version Released February 10, 2012, January 17, 2012.
[3] National Transportation Safety Board, Safety Recommendations A-04-29 through -33, April 23, 2004.
[4] Special Mission Airworthiness Assurance plan for Aerial Firefighting for FY 2010-2015, US Forest Service Fire and Aviation Management, January 31, 2009.
[5] Kamran Rokhsaz, Linda K. Kliment, and Richard B. Bramlette, "Usage and Maneuver Loads Monitoring of Heavy Air Tankers," DOT/FAA/AR-11/7, March 2011.
[6] Kliment, L.K., Rokhsaz, K., Nelson, J., Terning, B., and Weinstein, E.M., "Usage and Flight Loads Analysis of King Airs in Aerial Firefighting Missions," *AIAA Journal of Aircraft*, Vol. 52, pp. 910-916, 2015.
[7] Menon, A., Kliment, L.K., Rokhsaz, K., Nelson, J., and Terning, B., "Flight Loads and Atmospheric Turbulence Analysis from a Fleet of ASM/Lead Aircraft," AIAA-2015-1845, 56th AIAA/ASCE/AHS/ASC Structures, Structural Dynamics, and Materials Conference, 2015.
[8] Kliment, L.K., Rokhsaz, K., Nelson, J., and Terning, B., "Statistical Usage of BAe-146 and RJ-85 Air Tankers in Forest Service Operation," AIAA-2019-3573, 2019 AIAA Aviation and Aeronautics Forum and Exposition, June 2019.
[9] Rokhsaz, K., Kliment, L.K., Terning, B.R., and Nelson, J.A., "Flight Loads Spectra of a Fleet of Heavy Air Tankers," AIAA-2019-3364, 2019 AIAA Aviation and Aeronautics Forum and Exposition, June 2019.
[10] NWCG Airtanker Base Directory, PMS 507, National Wildfire Coordinating Group, April 2019.
[11] Naval Air Systems Command, "NATOPS Flight Manual; Navy Models EC-130G/Q Aircraft," NAVAIR 01-75GAE-1, March 1, 1969 with Change 1 August 27, 1969.
[12] Department of Transportation Federal Aviation Administration, "Type Certificate Date Sheet No. T00019LA," EC-130Q, Revision 2, May 2017.
[13] Department of Transportation Federal Aviation Administration, "Type Certificate Date Sheet No. A1SO," Lockheed 382, Revision 17, November 2019.
[14] Coulson Aviation, "Aircraft Flight Manual; Coulson EC-130Q," Report CAG 109, FAA Approved, August 2013.
[15] Etkin, B., *Dynamics of Flight, Stability and Control* – Second Edition, John Wiley & Sons, New York, New York, 1982.
[16] Dommasch, D. O., Sherby, S. S., and Connolly, T. F., *Airplane Aerodynamics* – Fourth Edition, Pitman Publishing Corporation, New York, New York, 1967.
[17] Roskam, Jan, *Airplane Flight Dynamics and Automatic Flight Controls – Part I*, Third Printing, DARcorporation, Lawrence, Kansas, 2001.
[18] Jones, T., Rustenburg, J. W., Skinn, D. A., Tipps, D. O., and DeFiore, T., "Statistical Data for the Boeing-747-400 Aircraft in Commercial Operations," FAA Report DOT/FAA/AR-04/44, January 2005.